Probabilistic dynamic-controlled latent variable model for pattern-space modelling and pattern-based stochastic model predictive control

Niannian Zheng*,†, Yuri A.W. Shardt*, Xiaoli Luan†, Fei Liu†

**Department of Automaton Engineering, Technical University of Ilmenau, 98693 Ilmenau, Germany*
†Department of Automation, Jiangnan University, 214122 Wuxi, China
(e-mail: zhengniannian@stu.jiangnan.edu.cn, yuri.shardt@tu-ilmenau.de, xlluan@jiangnan.edu.cn, fliu@jiangnan.edu.cn)

Abstract: Industrial processes are measured and controlled using high-dimensional process variables, but its overall operation is usually characterised by low-dimensional patterns. The changes in the pattern are dominated by three features: free motion, controlled motion, and uncertainty. In this paper, all three features are taken into consideration to propose a new probabilistic dynamic-controlled latent variable (PDCLV) model structure using a dynamic Bayesian network for process modelling in the pattern space. To this end, the linear dynamic system characterised by control inputs is introduced, and the expectation maximisation algorithm is specially designed for learning the PDCLV model. Benefitting from the dynamic causality between control inputs and the explicit modelling of the pattern, a method for pattern-based stochastic model predictive control (SMPC) is implemented successfully to realise process optimisation. A case study on an industrial boiler combustion process demonstrates the benefits of the proposed PDCLV structure for pattern-space modelling and pattern-based SMPC.

Keywords: **Dynamic controlled latent variable, pattern space modelling; dynamic Bayesian network; linear dynamic system with control inputs, expectation maximisation, stochastic model predictive control**

1. INTRODUCTION

With the wide use of hierarchical distributed control and digital measurements, industrial processes are usually measured and regulated by a large number of process variables (PVs) such as the temperature, pressure, and liquid level [1]. In engineering practice, there is often the problem that each PV is controlled based on the assumed normal process condition, but the operation of the complete process may still be poor [2]-[3]. By analyzing the geometric features of PVs, the reason for such a problem is that the PVs merely reflect the process behaviours in a decentralised, independent, and partial manner, while they are mutually correlated in the spatial structure [4]. Consequently, the holistic effect of the PVs and the overall running characteristics of the process are in accordance with the pattern which is embedded in the PVs geometrically and statistically, and describes the process in a centralised and latent way [5]-[7].

To characterize the operational pattern, researchers in multivariate statistical process monitoring resort to latent variable (LV) modelling methods such as principal component analysis (PCA) [8]-[9], independent component analysis (ICA) [10], canonical correlation analysis (CCA) [11]-[12], partial least squares (PLS) [13]-[14], and their extensions for special conditions (nonlinear, multimode, and batch processes) [15]-[17]. These methods can project high-dimensional PVs onto a low-dimensional pattern space that concentrates the main process information. In addition, these data-based methods do not need explicit knowledge about the process, while still using the available PV data.

In addition to spatial correlation, almost all PVs are dominated by process dynamics (free and controlled motions, the former derived from the inherent inertia of the process, that is, the autoregressive characteristics of the process, the latter driven by external control inputs), and contaminated by noise. Consequently, it will be more natural if a pattern can provide the dynamic description and probabilistic interpretation for the process. Unfortunately, the methods mentioned above are based on a spatial projection of the PVs, and thus, focus merely on the static and deterministic geometric relationships of the PVs.

To capture the process dynamics, many dynamic versions of the static LV models have been developed, which include two types of an augmented PV matrix with lagged measurements [18]-[21] and the structured dynamic LV with an autoregressive (AR) model [22]-[26]. The former performs a static projection onto the augmented PV matrix, and thus, poorly characterises the low-dimensional and dynamic pattern of the process [23]. The latter describes the pattern dynamic through the AR structure, which can fully capture the free motions of the PVs.

To deal with process uncertainty, many probabilistic counterparts of the static LV models have been put forward [27]-[30]. These methods focus on finding a generative model from the LVs to the PVs, which can interpret the deterministic spatial relationship between the PVs and the LVs, as well as the stochastic characteristics of the process. As well, a prominent advantage of the probabilistic LV structure is that the expectation-maximisation (EM) algorithm can be used to learn the model, which can greatly reduce the computational burden, particularly for high-dimensional PVs [29].

To simultaneously consider the dynamics and uncertainty, dynamic Bayesian networks (DBN) have been introduced for pattern modelling. As a typical DBN model, the linear dynamic system (LDS) uses continuous LVs sequences to describe the process dynamic relationships. Under the LDS, some researchers have achieved successful integrations of the AR structure and probabilistic generation model [31]-[36], and obtained the corresponding probabilistic dynamic LV (PDLV) modelling methods for pattern extraction. The advantages are i) eliminating the redundant dimensions in the PVs; ii) modelling the free motions of the process; and iii) interpreting the uncertain information in the PVs. However, since the LDS in the existing PDLV models uses the AR structure, the dynamic causality between the control inputs and the pattern remains unmodelled or implicit, which results in the impracticality of directly controlling and optimising the pattern.

To overcome this limitation, a probabilistic dynamic-controlled LV (PDCLV) modelling method is proposed in this paper for process pattern extraction and dynamic modelling. In this method, the LDS is characterised by the control inputs, while the AR with exogenous inputs (ARX) structure is used to describe the pattern dynamics. An EM algorithm is designed for learning the model under the new LDS framework. Thus, the proposed PDCLV model not only retains the advantages of the existing PDLV models, but also explicitly determines the dynamic causality between the control inputs and pattern. Thus, the pattern can be controlled directly by the manipulated inputs. In addition, the pattern can describe the whole process in a more lumped but concise way than the PVs, providing a good opportunity for overall process optimisation. Stochastic model predictive control (SMPC) [37] is used in this paper and set at the constraint control layer to realize process pattern optimisation.

2. PROBABILISTIC DYNAMIC-CONTROLLED LATENT VARIABLE MODELLING

2.1. PDCLV Model Structure

In this paper, the extracted LVs $\mathbf{t} \in \mathbb{R}^m$ are assumed to be m-variate Gaussian and used to characterise the process operation pattern. For the static spatial relationships and uncertainties, the n-dimensional measured PVs are denoted as $\mathbf{x}$ and regarded as the generative results of linear combination of $\mathbf{t}$ plus an additive noise $\mathbf{e} \in \mathbb{R}^n$. In addition, considering both the free and controlled dynamic relationships of the process, the LDS is introduced and characterised by control inputs $\mathbf{u} \in \mathbb{R}^d$. Consequently, the proposed PDCLV structure consists of a Gaussian ARX time-series model and a linear Gaussian observation model, that can be written as

$$\mathbf{t}_{k+1} = \mathbf{A}\mathbf{t}_k + \mathbf{B}\mathbf{u}_k + \mathbf{w}_k \tag{1}$$

$$\mathbf{x}_k = \mathbf{Q}\mathbf{t}_k + \mathbf{e}_k \tag{2}$$

where k is the time instant. For the ARX model (1), the white noise $\mathbf{w}_k \in \mathbb{R}^m$ follows a Gaussian distribution with a mean of zero and a variance $\mathbf{\Phi}_w \in \mathbb{R}^{m\times m}$; the transition matrix $\mathbf{A} \in \mathbb{R}^{m\times m}$ describes the free motions of the pattern; the input matrix $\mathbf{B} \in \mathbb{R}^{m\times d}$ expresses the dynamic-causal relationships between the control inputs $\mathbf{u}_k$ and the successive pattern $\mathbf{t}_{k+1}$. In the generation model (2), $\mathbf{Q} \in \mathbb{R}^{n\times m}$ is the emission matrix of the PVs, reflecting the static and deterministic relationships between the LVs and the pattern in the geometric structure; $\mathbf{e}_k$ follows a n-variate Gaussian distribution with a mean of zero and a variance $\mathbf{\Phi}_e \in \mathbb{R}^{n\times n}$, providing the probabilistic interpretation for the PVs. It should be noted that, in general, the pattern $\mathbf{t}_k$ is not a state vector unless all latent components have first-order dynamics [38]. Therefore, the pattern dynamic equation is usually not the state-space representation as model (1), but a vector time-series model with ARX structure, which can be generally expressed as

$$\mathbf{t}_k = \sum_{i=1}^{s_1} \mathbf{A}_i \mathbf{t}_{k-i} + \sum_{j=1}^{s_2} \mathbf{B}_j \mathbf{u}_{k-j} + \mathbf{w}_k \tag{3}$$

where s_1 and s_2 are, respectively, the AR and controlled dynamic orders; $\mathbf{A}_i \in \mathbb{R}^{m\times m}$ and $\mathbf{B}_j \in \mathbb{R}^{m\times d}$ for $i = 1, \ldots, s_1$ and $j=1, \ldots, s_2$ and the model parameters. For the sake of clarity and convenience, the theoretical derivations of this paper take the first-order case (1) as an example, and the derivation of the generalized model (3) can be easily extended.

The graphical structure of the proposed PDCLV model is show in Figure 1.

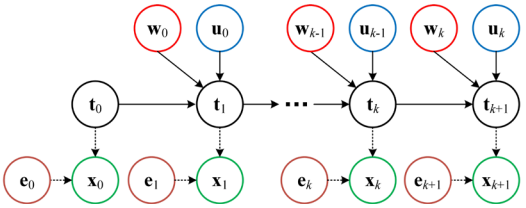

Figure 1. Graphical structure of the PDCLV model

From Figure 1, it can be seen that: i) there is always a path connecting any two PVs measured at different instants via the patterns, and this connection is never blocked; ii) from the spatial perspective, pattern $\mathbf{t}$ interprets the main information of the PVs $\mathbf{x}$, and the noise $\mathbf{e}$ interprets the remaining random part; and iii) from the time perspective, the pattern sequence has the Markov property, and $\mathbf{t}_k$ collects and summarises all the previous information (free and controlled dynamics, noise characteristics, and spatial structure relationships).

To obtain the inference process for the pattern, the prior distribution of $\mathbf{t}_0$ is assumed to be Gaussian with a mean of $\mathbf{h}_0$ and a variance of $\mathbf{H}_0$ with the probability density function (pdf)

$$p(\mathbf{t}_0) = \frac{1}{\sqrt{\det(2\pi\mathbf{H}_0)}} \times \exp\left\{-\frac{1}{2}(\mathbf{t}_0 - \mathbf{h}_0)^{\mathrm{T}} \mathbf{H}_0^{-1} (\mathbf{t}_0 - \mathbf{h}_0)\right\} \tag{4}$$

Based on the linear Gaussian ARX model (1) and linear Gaussian observation model, and the fact that a Gaussian variable under a linear transformation is another Gaussian, the conditional pdfs of $\mathbf{t}_k$ and $\mathbf{x}_k$ are given by (5) and (6).

$$p(\mathbf{t}_k \,|\mathbf{t}_{k-1}, \mathbf{u}_{k-1}) = \frac{1}{\sqrt{\det(2\pi\mathbf{\Phi}_w)}} \times \exp\left\{-\frac{1}{2}(\mathbf{t}_k - \mathbf{A}\mathbf{t}_{k-1} - \mathbf{B}\mathbf{u}_{k-1})^{\mathrm{T}} \mathbf{\Phi}_w^{-1} (\mathbf{t}_k - \mathbf{A}\mathbf{t}_{k-1} - \mathbf{B}\mathbf{u}_{k-1})\right\} \tag{5}$$

$$p\left(\mathbf{x}_k \left| \mathbf{t}_k \right.\right) = \frac{1}{\sqrt{\det\left(2\pi\mathbf{\Phi}_e\right)}} \times \exp\left\{-\frac{1}{2}\left(\mathbf{x}_k - \mathbf{Q}\mathbf{t}_k\right)^{\mathrm{T}} \mathbf{\Phi}_e^{-1}\left(\mathbf{x}_k - \mathbf{Q}\mathbf{t}_k\right)\right\} \tag{6}$$

In addition, the control inputs are assumed to be constant at any instant. Therefore, $\mathbf{u}_k$ can be considered to follow a special distribution with a mean of $\mathbf{u}_k$ and a variance of zero, whose pdf is

$$p\left(\mathbf{u}_k\right) = 1 \tag{7}$$

The assumptions on $\mathbf{u}$ are natural and reasonable, which can be supported by the fact that this paper is devoted to exploring how the pattern is affected by the values (measurements) rather than the variance of $\mathbf{u}$.

2.2. The Expectation-Maximisation Algorithm

Based on the pdfs (4) to (7), the joint probability for the sequences of $\mathbf{t}_k$, $\mathbf{x}_k$, and $\mathbf{u}_k$ can be derived to give the log-likelihood function in (8).

$$\begin{aligned}
&\ln p\left(\mathbf{x}_{0:N}, \mathbf{u}_{0:N}, \mathbf{t}_{0:N}\right) \\
&= \ln\left[p\left(\mathbf{u}_0\right) p\left(\mathbf{t}_0\right) p\left(\mathbf{x}_0 \left| \mathbf{t}_0 \right.\right) \prod_{k=1}^{N} p\left(\mathbf{u}_k\right) p\left(\mathbf{t}_k \left| \mathbf{x}_{k-1}, \mathbf{u}_{k-1} \right.\right) p\left(\mathbf{x}_k \left| \mathbf{t}_k \right.\right) \right] \\
&= \ln p\left(\mathbf{t}_0\right) + \sum_{k=0}^{N} \ln p\left(\mathbf{u}_k\right) + \sum_{k=0}^{N} \ln p\left(\mathbf{x}_k \left| \mathbf{t}_k \right.\right) + \sum_{k=1}^{N} \ln p\left(\mathbf{t}_k \left| \mathbf{x}_{k-1}, \mathbf{u}_{k-1} \right.\right)
\end{aligned} \tag{8}$$

where the first equality is obtained by the chain rule; $N+1$is the length of data used for model learning; $\mathbf{x}_{0:N}$, $\mathbf{u}_{0:N}$ and $\mathbf{t}_{0:N}$ are the sequences for the three variables measured from time zero to N. The log-likelihood function (8) has actually been determined following the pdfs (4)-(7). Then, the parameter to be estimated is $\mathbf{\Theta} = \{\mathbf{A}, \mathbf{B}, \mathbf{Q}, \mathbf{\Phi}_w, \mathbf{\Phi}_e, \mathbf{h}_0, \mathbf{H}_0\}$. To improve the efficiency and reduce the computational burden of model estimation, the EM algorithm is introduced in this paper and designed under the PDCLV structure, which consists of the expectation step (E-step) and the maximisation step (M-step). For the given data sequences $\mathbf{x}_{0:N}$ and $\mathbf{u}_{0:N}$, the expectation of the log-likelihood function (8) is given by (9).

$$\begin{aligned}
&E\left[\ln p\left(\mathbf{x}_{0:N}, \mathbf{u}_{0:N}, \mathbf{t}_{0:N} \left| \mathbf{\Theta} \right.\right)\right] \\
&= -\frac{1}{2}\left\{\ln\left|\mathbf{H}_0\right| + E\left(\mathbf{t}_0^{\mathrm{T}} \mathbf{H}_0^{-1} \mathbf{t}_0\right) - E\left(\mathbf{t}_0^{\mathrm{T}}\right)\mathbf{H}_0^{-1}\mathbf{h}_0 - \mathbf{h}_0^{\mathrm{T}}\mathbf{H}_0^{-1}E\left(\mathbf{t}_0\right) + \mathbf{h}_0^{\mathrm{T}}\mathbf{H}_0^{-1}\mathbf{h}_0\right\} \\
&\quad -\frac{1}{2}\left\{(N+1)\ln\left|\mathbf{\Phi}_e\right| + \sum_{k=0}^{N}\left[\mathbf{x}_k^{\mathrm{T}}\mathbf{\Phi}_e^{-1}\mathbf{x}_k - \mathbf{x}_k^{\mathrm{T}}\mathbf{\Phi}_e^{-1}\mathbf{Q}E\left(\mathbf{t}_k\right) - E\left(\mathbf{t}_k^{\mathrm{T}}\right)\mathbf{Q}^{\mathrm{T}}\mathbf{\Phi}_e^{-1}\mathbf{x}_k + E\left(\mathbf{t}_k^{\mathrm{T}}\mathbf{Q}^{\mathrm{T}}\mathbf{\Phi}_e^{-1}\mathbf{Q}\mathbf{t}_k\right)\right]\right\} \\
&\quad -\frac{1}{2}\left\{N\ln\left|\mathbf{\Phi}_w\right| + \sum_{k=1}^{N}\left[E\left(\mathbf{t}_k^{\mathrm{T}}\mathbf{\Phi}_w^{-1}\mathbf{t}_k\right) - E\left(\mathbf{t}_k^{\mathrm{T}}\mathbf{\Phi}_w^{-1}\mathbf{A}\mathbf{t}_{k-1}\right) - E\left(\mathbf{t}_k^{\mathrm{T}}\right)\mathbf{\Phi}_w^{-1}\mathbf{B}\mathbf{u}_{k-1} - E\left(\mathbf{t}_{k-1}^{\mathrm{T}}\mathbf{A}^{\mathrm{T}}\mathbf{\Phi}_w^{-1}\mathbf{t}_k\right)\right.\right. \\
&\quad \left.\left. + E\left(\mathbf{t}_{k-1}^{\mathrm{T}}\mathbf{A}^{\mathrm{T}}\mathbf{\Phi}_w^{-1}\mathbf{A}\mathbf{t}_{k-1}\right) + E\left(\mathbf{t}_{k-1}^{\mathrm{T}}\right)\mathbf{A}^{\mathrm{T}}\mathbf{\Phi}_w^{-1}\mathbf{B}\mathbf{u}_{k-1} - \mathbf{u}_{k-1}^{\mathrm{T}}\mathbf{B}^{\mathrm{T}}\mathbf{\Phi}_w^{-1}E\left(\mathbf{t}_k\right) + \mathbf{u}_{k-1}^{\mathrm{T}}\mathbf{B}^{\mathrm{T}}\mathbf{\Phi}_w^{-1}\mathbf{A}E\left(\mathbf{t}_{k-1}\right) + \mathbf{u}_{k-1}^{\mathrm{T}}\mathbf{B}^{\mathrm{T}}\mathbf{\Phi}_w^{-1}\mathbf{B}\mathbf{u}_{k-1}\right]\right\} \\
&\quad -\frac{1}{2}(N+1)(m+n)\ln(2\pi)
\end{aligned} \tag{9}$$

In the M-step, the new estimate $\mathbf{\Theta}^{new}$ can be obtained by maximizing $E[\ln p(\mathbf{x}_{0:N}, \mathbf{u}_{0:N}, \mathbf{t}_{0:N}|\mathbf{\Theta})]$, which is given as

$$\mathbf{\Theta}^{new} = \arg\max_{\mathbf{\Theta}} E\left[\ln p\left(\mathbf{x}_{0:N}, \mathbf{u}_{0:N}, \mathbf{t}_{0:N} \left| \mathbf{\Theta} \right.\right)\right]_{p\left(\mathbf{t}_{0:N} \left| \mathbf{x}_{0:N}, \mathbf{u}_{0:N}, \mathbf{\Theta}^{old} \right.\right)} \tag{10}$$

where $p(\mathbf{t}_{0:N}|\ \mathbf{x}_{0:N}, \mathbf{u}_{0:N}, \mathbf{\Theta}^{old})]$ is the posterior distribution of the pattern sequence under the previous estimate $\mathbf{\Theta}^{old}$. Considering the sensitivity of EM algorithm to the initial condition and to avoid the non-uniqueness issue, multiple trials can be carried out on the training set for model training. Then, the model accuracy can be verified using the test set, and finally, the best model is retained.

As a result, the optimal estimate $\mathbf{\Theta}^{opt}$ can be obtained by iteratively updating and recalculating the E-step and M-step until convergence. Then, the PDCLV model defined in this paper can be obtained, which can: i) explain the static and deterministic structural relationships between the hidden pattern and the measured PVs in the geometric space, which is formulated by the emission matrix $\mathbf{Q}$ in model (2); ii) interpret the random characteristics of the PVs, since the Gaussian noise $\mathbf{e}$ is incorporated into the PDCLV structure and the corresponding distribution information is estimated; iii) capture the free motions of the PVs, which is modelled by pattern transition matrix $\mathbf{A}$; and iv) explicitly establish the dynamic causality between the control inputs and the pattern, which is modelled by the input matrix $\mathbf{B}$. As well, an estimate of the Gaussian distribution for $\mathbf{w}$ can make the description of pattern dynamics more objective and natural considering the fact that the processes are disturbed by noise.

3. PATTERN-BASED STOCHASTIC MODEL PREDICTIVE CONTROL

3.1. Basic Framework for Pattern Control

From the above discussions, it can be seen that compared with the existing PDLV structure, the proposed PDCLV model has the advantage that the influence of control inputs on the pattern is quantitatively and explicitly modelled. Therefore,

the pattern dynamic equation formulated by the Gaussian ARX model (1) can be used for describing the process dynamic characteristics as well as implementing a direct way to control the pattern. This section seeks to discuss the application of pattern-based process control. Figure 2 shows the framework for this proposed control strategy.

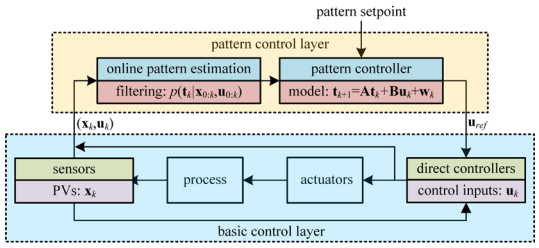

Figure 2. The framework for pattern-based process control

All the variables in Figure 2 are available online. It can be seen from Figure 2 that one of the important functions of the pattern control layer is to provide the input references $\mathbf{u}_{ref}$ for the basic control layer, which is the same as a cascade control strategy.

As well, compared with the PVs, the pattern describes the whole process from a more global and centralised perspective. Thus, it can provide a good opportunity for overall process optimisation, for example, by deriving the pattern setpoint from the plant-level optimisation problems (usually economic objectives), while the pattern control layer will provide the optimal references for the basic control layer.

Furthermore, since the constraints existing in the PVs must also be imposed on the pattern space, and the pattern dynamic equation contains additive disturbances, SMPC is the natural strategy for pattern control.

3.2. Pattern Stochastic Model Predictive Control

In this section, the SMPC proposed in [37] is introduced, and presented in detail. Without a loss of generality, the zero-targeted tracking problem is discussed here, because any other constant tracking problem can be transformed into the zero case by defining the deviation between the pattern and the setpoint as the new pattern.

Based on model (1) and the superposition principle for a linear system, at any time k and for $i = 0, 1,\ldots$, the pattern dynamic predictions can be decomposed into the nominal part

$$\overline{\mathbf{t}}_{k+i+1} = \mathbf{A}\overline{\mathbf{t}}_{k+i} + \mathbf{B}\overline{\mathbf{u}}_{k+i} \tag{11}$$

and the pattern dynamic error $\boldsymbol{\varepsilon}_k = \mathbf{t}_k - \overline{\mathbf{t}}_k$, which evolves as

$$\boldsymbol{\varepsilon}_{k+i+1} = \boldsymbol{\Phi}\boldsymbol{\varepsilon}_{k+i} + \mathbf{w}_{k+i} \tag{12}$$

under the pattern controller

$$\mathbf{u}_{k+i} = \mathbf{K}\mathbf{t}_{k+i} + \boldsymbol{\lambda}_{k+i} \tag{13}$$

and its nominal component

$$\overline{\mathbf{u}}_{k+i} = \mathbf{K}\overline{\mathbf{t}}_{k+i} + \boldsymbol{\lambda}_{k+i} \tag{14}$$

where $\boldsymbol{\lambda}_{k+i} \in \mathbb{R}^d$, $i = 0, 1,\ldots L-1$ are the decision variables for the online SMPC optimisation, and $\boldsymbol{\lambda}_{k+i} = 0$ for $i \geq L$ with L a finite prediction horizon. $\boldsymbol{\Phi} = \mathbf{A}+\mathbf{B}\mathbf{K}$ is a prestabilising matrix. In this paper, the linear feedback gain $\mathbf{K}$ is selected as the linear quadratic regulator (LQR). In addition, it is assumed that $\mathbf{w}_k$ is bounded and lies in the compact convex polyhedron

$$\mathbb{W} \triangleq \left\{\mathbf{w} \in \mathbb{R}^m \mid\mid \mathbf{w} \mid \leq \sigma, \sigma = [\sigma_1, \cdots, \sigma_m]^{\mathrm{T}}\right\}$$

where $|\cdot|$ is an elementwise comparison. The above boundedness assumption on $\mathbf{w}_k$ is reasonable and agrees with reality, since for most processes the probability that the additive disturbance exceeds an arbitrarily large threshold is zero.

The pattern is subjected to probabilistic constraints such that

$$p\left(\mathbf{g}^{\mathrm{T}}\mathbf{t}_{k+i} \leq h\right) \geq p_c \tag{15}$$

where $\mathbf{g} \in \mathbb{R}^m$, $0 \leq p_c \leq 1$, and h is the constraint boundary. The pattern SMPC determines the sequence $\boldsymbol{\eta}_k = [\boldsymbol{\lambda}_k^{\mathrm{T}}, \ldots, \boldsymbol{\lambda}_{k+L-1}^{\mathrm{T}}]$ that minimises the expected cost

$$J = \sum_{i=0}^{\infty} \mathbb{E}\left\{\mathbf{t}_{k+i}^{\mathrm{T}}\mathbf{W}_{\mathbf{t}}\mathbf{t}_{k+i} + \mathbf{u}_{k+i}^{\mathrm{T}}\mathbf{W}_{\mathbf{u}}\mathbf{u}_{k+i} - l_{ssc}\right\} \tag{16}$$

where l_{ssc} is the steady cost defined as

$$l_{ssc} = \lim_{i\to\infty} \mathbb{E}\left\{\mathbf{t}_{k+i}^{\mathrm{T}}\mathbf{W}_{\mathbf{t}}\mathbf{t}_{k+i} + \mathbf{u}_{k+i}^{\mathrm{T}}\mathbf{W}_{\mathbf{u}}\mathbf{u}_{k+i}\right\} \tag{17}$$

and $\mathbf{W}_{\mathbf{t}}$ and $\mathbf{W}_{\mathbf{u}}$ are the weighting matrices for respectively the pattern and control inputs.

For rolling optimisation, the probabilistic constraints (15) will be satisfied and the recursive feasibility will be guaranteed if and only if

$$\mathbf{g}^{\mathrm{T}}\boldsymbol{\Phi}^i\overline{\mathbf{t}}_k + \mathbf{g}^{\mathrm{T}}\mathbf{H}_i\boldsymbol{\eta}_k \leq h - \beta_i, i = 1, 2, \cdots \tag{18}$$

where $\mathbf{H}_i$ is defined as

$$\mathbf{H}_i \triangleq \begin{cases}\left[\boldsymbol{\Phi}^{i-1}\mathbf{B}, \cdots, \mathbf{B}, \mathbf{0}, \cdots, \mathbf{0}\right], i = 1, \cdots, L-1\\ \left[\boldsymbol{\Phi}^{i-1}\mathbf{B}, \cdots, \boldsymbol{\Phi}^{i-L}\mathbf{B}\right], i = L, L+1, \cdots\end{cases} \tag{19}$$

and β_i is selected as the maximum element of the i^{th} column of the following matrix

$$\boldsymbol{\Gamma} = \begin{bmatrix}\gamma_1 & \gamma_2 & \gamma_3 & \gamma_4 & \cdots\\ 0 & \gamma_1+\xi_1 & \gamma_2+\xi_2 & \gamma_3+\xi_3 & \cdots\\ \vdots & 0 & \gamma_1+\xi_1+\xi_2 & \gamma_2+\xi_2+\xi_3 & \cdots\\ \vdots & \vdots & 0 & \gamma_1+\xi_1+\xi_2+\xi_3 & \cdots\\ \vdots & \vdots & \vdots & 0 & \ddots\end{bmatrix} \tag{20}$$

γ_i is the confidence boundary such that

$$p\left\{\mathbf{g}^{\mathrm{T}}\boldsymbol{\varepsilon}_{k+i} \leq \gamma_i\right\} = p\left\{\mathbf{g}^{\mathrm{T}}\left(\boldsymbol{\Phi}^{i-1}\mathbf{w}_k + \cdots + \mathbf{w}_{k+i-1}\right) \leq \gamma_i\right\} = p_c \tag{21}$$

and ξ_i the worst case given by

$$\xi_i = \max_{\mathbf{w}\in\mathbb{W}} \mathbf{g}^{\mathrm{T}}\boldsymbol{\Phi}^i\mathbf{w} \tag{22}$$

For the computability and tractability of online SMPC optimisation, the infinite constraints (18) are transformed into finite terms by computing the terminal conditions

$$\begin{aligned}\mathbb{T}_L \triangleq \Big\{\overline{\mathbf{t}}_L \mid\; & \mathbf{g}^{\mathrm{T}}\boldsymbol{\Phi}^l\overline{\mathbf{t}}_L \leq h - \beta_{L+l}, l = 1, \cdots, \hat{L}\\ & \mathbf{g}^{\mathrm{T}}\boldsymbol{\Phi}^l\overline{\mathbf{t}}_L \leq h - \overline{\beta}, l = \hat{L}+1, \cdots, \hat{L}+l^*\Big\}\end{aligned} \tag{23}$$

where $\bar{\beta}$ is a certain supremum of β_i, and the value of $\mathbb{T}_L$ can be determined according to Gilbert and Tan [39].

The online pattern SMPC optimisation problem $\mathcal{P}(\boldsymbol{\eta}_k)$ at time instant k can be summarised as

$$\begin{aligned}
&\boldsymbol{\eta}_k^* = \arg\min\{J\} \\
&\text{s.t. } \bar{\mathbf{t}}_k = \mathbf{t}_k \\
&\quad \mathbf{g}^{\mathrm{T}}\boldsymbol{\Phi}^i\bar{\mathbf{t}}_k + \mathbf{g}^{\mathrm{T}}\mathbf{H}_i\boldsymbol{\eta}_k \le h - \beta_i, i = 1,\cdots,L-1 \\
&\quad \mathbf{g}^{\mathrm{T}}\boldsymbol{\Phi}^L\bar{\mathbf{t}}_k + \mathbf{g}^{\mathrm{T}}\mathbf{H}_L\boldsymbol{\eta}_k \in \mathbb{T}_L \\
&\quad \begin{cases} \mathbf{u}_{k+i} = \mathbf{K}\mathbf{t}_{k+i} + \boldsymbol{\lambda}_{k+i} \\ \mathbf{t}_{k+i+1} = \mathbf{A}\mathbf{t}_{k+i} + \mathbf{B}\mathbf{u}_{k+i} + \mathbf{w}_{k+i} \end{cases}, i = 0,1,\cdots
\end{aligned} \tag{24}$$

After each optimisation, one-step-ahead control $\mathbf{u}_k = \mathbf{K}\mathbf{t}_k + \boldsymbol{\lambda}_k^*$ is applied to the pattern dynamic equation (1).

4. INDUSTRIAL CASE STUDY

The combustion process is an important part of an industrial boiler, related closely to the operation performance of the steam-water system and the efficiency of the whole boiler. The existing monitoring and control for this process are based on two key strategies: to carry out single-loop-based key PVs control; and to extract and observe the statistical operation pattern so as to achieve overall status monitoring. In this case study, the proposed PDCLV modelling method is applied to the pattern modelling and pattern SMPC of the industrial boiler combustion process, which overcomes the limitation that the PVs-based control cannot carry out collaborative regulation on the overall pattern, as well as the limitation that the existing LV modelling method is unable to control the combustion process pattern.

As shown in Table 1, the combustion process studied in this paper is measured and controlled by 19 key PVs. There are three manipulated inputs: air intake volume of the furnace, air induced volume, and the speed of the coal feeder representing the fuel flow.

Table 1. Key Controlled and Measured PVs in the Industrial Boiler Combustion Process

PV	description	PV	description
x_1	furnace differential pressure	x_{11}	FGP at the outlet of the HTS
x_2	furnace lower pressure	x_{12}	FGT at the inlet of the LTS
x_3	furnace outlet pressure	x_{13}	FGP at the inlet of the LTS
x_4	furnace upper temperature	x_{14}	FGT at the outlet of the LTS
x_5	furnace middle temperature	x_{15}	FGP at the outlet of the LTS
x_6	furnace lower temperature	x_{16}	material temperature of the return bed
x_7	FGT at the furnace outlet	x_{17}	water temperature at the inlet of the IHE
x_8	FGT at the inlet of the HTS	x_{18}	FGT at the outlet of the IHE
x_9	FGP at the inlet of the HTS	x_{19}	FGP at the outlet of the IHE
x_{10}	FGT at the outlet of the HTS		

(Abbreviations: FGT: flue gas temperature; FGP: flue gas pressure; HTS: high temperature superheater; LTS: low temperature superheater; and IHE: import header of the economiser)

In a single steam load, 591 data samples were collected, which were divided into a training set (291 samples) and a test set (the remaining 300 samples). Based on the training data, pattern modelling can be implemented using the PDCLV model. For comparison analysis, PDLV modelling [35] was used to model the combustion process.

The cross-correlation between the control inputs and the final retained two LVs are shown in Figure 3, where the title c_{ij} shows that this subfigure considers the cross-correlation between the j-th control input and the i-th latent variable.

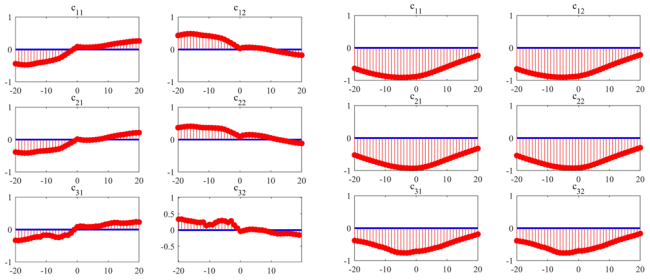

(a) PDLV *(b) PDCLV*

Figure 3. Cross-correlation of the control inputs and LVs

From Figure 3, it can be seen that the cross-correlation of PDLV is weaker and more disordered compared with that of the PDCLV method, which shows that the proposed PDCLV method can better extract and determine the dynamic-causal

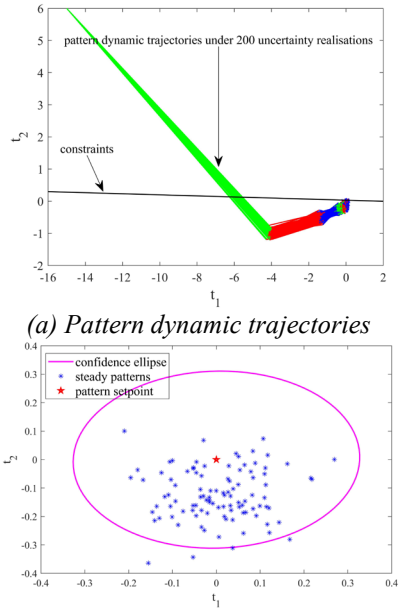

(a) Pattern dynamic trajectories

(b) Steady pattern distribution

Figure 4. Pattern dynamic trajectories

relationships between the control inputs and pattern of the industrial boiler combustion process.

Of note, benefiting from the fact that the dynamic-causal relationship between the control inputs and pattern is explicitly modelled, it is now feasible to control the combustion process pattern. The following case study will provide a concrete implementation.

After pattern dynamic modelling, the pattern SMPC is implemented. First, the combustion process operates stably under a certain load. Then, the new steam load requires the combustion process pattern to operate around a new setpoint. Using pattern SMPC, automatic pattern tracking can be achieved, whose dynamic trajectories and steady distribution (within the 95% confidence ellipse) under 200 uncertainty realisations is shown in Figure 4.

It can be seen that the pattern dynamic trajectories satisfy the constraints and converges to the region centred by the setpoint. Thus, SMPC successfully implements pattern tacking.

REFERENCES

[1] J. M. Guerrero, M. Chandorkar, T. Lee and P. C. Loh, "Advanced control architectures for intelligent microgrids-Part I: Decentralized and fierarchical control," IEEE Trans. Ind. Electron., vol. 60, no. 4, pp. 1254-1262, Apr. 2013.

[2] J. F. MacGregor and T. Kourti, "Statistical process control of multivariate processes," Control Eng. Pract., vol. 3, no. 3, pp. 403-414, Mar. 1995.

[3] Q. P. He and J. Wang, "Statistical process monitoring as a big data analytics tool for smart manufacturing," J. Process Control., vol. 67, pp. 35-43, Jul. 2018.

[4] J. C. Wang, Y. B. Zhang, H. Cao, and W. Z. Zhu, "Dimension reduction method of independent component analysis for process monitoring based on minimum mean square error," J. Process Control., vol. 22, no. 2, pp. 477-487, Feb. 2012.

[5] C. Xu, S. Y. Zhao, and F. Liu, "Distributed plant-wide process monitoring based on PCA with minimal redundancy maximal relevance," Chemom. Intell. Lab. Syst., vol. 169, no. 15, pp. 53-63, Oct. 2017.

[6] Z. B. Zhu, Z. H. Song, and A. Palazoglu, "Process pattern construction and multi-mode monitoring," J. Process Control., vol. 22, no. 1, pp. 247-262, Jan. 2012.

[7] X. G. Deng and X. M. Tian, "Nonlinear process fault pattern recognition using statistics kernel PCA similarity factor," Neurocomputing, vol. 121, no. 9, pp. 298-308, Dec. 2013.

[8] B. Song and H. Shi, "Fault detection and classification using quality-supervised double-layer method," IEEE Trans. Ind. Electron., vol. 65, no. 10, pp. 8163-8172, Oct. 2018.

[9] Q. Jiang, X. Yan and B. Huang, "Performance-driven distributed PCA process monitoring based on fault-relevant variable selection and Bayesian inference," IEEE Trans. Ind. Electron., vol. 63, no. 1, pp. 377-386, Jan. 2016.

[10] Y. Zhang, W. Du and X. Li, "Observation and detection for a class of industrial systems," IEEE Trans. Ind. Electron., vol. 64, no. 8, pp. 6724-6731, Aug. 2017.

[11] Z. Chen, S. X. Ding, T. Peng, C. Yang and W. Gui, "Fault detection for non-Gaussian processes using generalized canonical correlation analysis and randomized algorithms," IEEE Trans. Ind. Electron., vol. 65, no. 2, pp. 1559-1567, Feb. 2018.

[12] Q. Jiang, S. X. Ding, Y. Wang and X. Yan, "Data-driven distributed local fault detection for large-scale processes based on the GA-regularized canonical correlation analysis," IEEE Trans. Ind. Electron., vol. 64, no. 10, pp. 8148-8157, Oct. 2017.

[13] S. Yin, X. Zhu and O. Kaynak, "Improved PLS focused on key performance indicator-related fault diagnosis," IEEE Trans. Ind. Electron., vol. 62, no. 3, pp. 1651-1658, Mar. 2015.

[14] S. J. Zhao, J. Zhang, and Y. M. Xu, "Performance monitoring of processes with multiple operating modes through multiple PLS models," J. Process Control., vol. 16, no. 7, pp. 763-772, Aug. 2006.

[15] Z. Zhou, C. Wen and C. Yang, "Fault isolation based on k-nearest neighbor rule for industrial processes," IEEE Trans. Ind. Electron., vol. 63, no. 4, pp. 2578-2586, Apr. 2016.

[16] S. Yin, X. Xie and W. Sun, "A nonlinear process monitoring approach with locally weighted learning of available data," IEEE Trans. Ind. Electron., vol. 64, no. 2, pp. 1507-1516, Feb. 2017.

[17] K. Peng, K. Zhang, B. You, J. Dong and Z. Wang, "A quality-based nonlinear fault diagnosis framework focusing on industrial multimode batch processes," IEEE Trans. Ind. Electron., vol. 63, no. 4, pp. 2615-2624, Apr. 2016.

[18] J. Jiao, H. Yu and G. Wang, "A quality-related fault detection approach based on dynamic least squares for process monitoring," IEEE Trans. Ind. Electron., vol. 63, no. 4, pp. 2625-2632, Apr. 2016.

[19] W. F. Ku, R. H. Storer, and C. Georgakis, "Disturbance detection and isolation by dynamic principal component analysis," Chemom. Intell. Lab. Syst., vol. 30, no. 1, pp. 179-196, Nov. 1995.

[20] J. Huang and X. F. Yan, "Dynamic process fault detection and diagnosis based on dynamic principal component analysis, dynamic independent component analysis and Bayesian inference," Chemom. Intell. Lab. Syst., vol. 148, no. 15, pp. 115-127, Nov. 2015.

[21] J. Shang and M. Chen, "Recursive dynamic transformed component statistical analysis for fault detection in dynamic processes," IEEE Trans. Ind. Electron., vol. 65, no. 1, pp. 578-588, Jan. 2018.

[22] G. Li, S. J. Qin and D. Zhou, "A new method of dynamic latent variable modelling for process monitoring," IEEE Trans. Ind. Electron., vol. 61, no. 11, pp. 6438-6445, Nov. 2014.

[23] Y. N. Dong and S. J. Qin, "A novel dynamic PCA algorithm for dynamic data modelling and process monitoring," J. Process Control., vol. 67, pp. 1-11, Jul. 2018.

[24] Y. N. Dong and S. J. Qin, "Dynamic latent variable analytics for process operations and control," Comput. Chem. Eng., vol. 114, no. 9, pp. 69-80, Jun. 2018.

[25] Y. N. Dong and S. J. Qin, "Regression on dynamic PLS structures for supervised learning of dynamic data," J. Process Control., vol. 68, pp. 64-72, Aug. 2018.

[26] Y. N. Dong and S. J. Qin, "Dynamic inner canonical correlation and causality analysis for high dimensional time series data," IFAC-Papers OnLine. vol. 68, no. 18, pp. 476-481, 2018.

[27] D. Kim, and I. B. Lee, "Process monitoring based on probabilistic PCA," Chemom. Intell. Lab. Syst., vol. 67, no. 2, pp. 109-123, Aug. 2003.

[28] L. Zhou, J. H. Chen, Z. H. Song, Z. Q. Ge, and A. M. Miao, "Probabilistic latent variable regression model for process-quality monitoring," Chem. Eng. Sci., vol. 116, pp. 296-305, Sep. 2014.

[29] Z. Q. Ge, "Process data analytics via probabilistic latent variable models: A tutorial review," Ind. Eng. Chem. Res., vol. 57, no. 38, pp. 12646-12661, Aug. 2018.

[30] R. Raveendran, H. Kodamana, and B. Huang, "Process monitoring using a generalized probabilistic linear latent variable model," Automatica., vol. 96, pp. 73-83, Oct. 2018.

[31] L. Zhou, G. Li, Z. Song and S. J. Qin, "Autoregressive dynamic latent variable models for process monitoring," IEEE Trans. Control Syst. Technol., vol. 25, no. 1, pp. 366-373, Jan. 2017.

[32] Y. Ma and B. Huang, "Bayesian learning for dynamic feature extraction with application in soft sensing," IEEE Trans. Ind. Electron., vol. 64, no. 9, pp. 7171-7180, Sept. 2017.

[33] J. L. Zhu, Z. Q. Ge, and Z. H. Song, "Bayesian robust linear dynamic system approach for dynamic process monitoring," J. Process Control., vol. 40, pp. 62-77, Apr. 2016.

[34] Z. Q. Ge and X. R. Chen, "Supervised linear dynamic system model for quality related fault detection in dynamic processes," J. Process Control., vol. 44, pp. 224-235, Aug. 2016.

[35] Z. Q. Ge and X. R. Chen, "Dynamic probabilistic latent variable model for process data modelling and regression application," IEEE Trans. Control Syst. Technol., vol. 27, no. 1, pp. 323-331, Jan. 2019.

[36] J. Zhu, Z. Q. Ge and Z. H. Song, "HMM-driven robust probabilistic principal component analyzer for dynamic process fault classification," IEEE Trans. Ind. Electron., vol. 62, no. 6, pp. 3814-3821, Jun. 2015.

[37] B. Kouvaritakis, M. Cannon, S. V. Raković, Q. F. Cheng, " Explicit use of probabilistic distributions in linear predictive control," Automatica, vol. 46, no. 10, pp. 1719-1724, Oct. 2010.

[38] S. J. Qin, Y. N. Dong g, Q. Q. Zhu, J. Wang and Q. Liu, " Bridging systems theory and data science: A unifying review of dynamic latent variable analytics and process monitoring," Annu Rev Control, vol. 50, pp. 29-48, Oct. 2020.

[39] E. G. Gilbert and K. T. Tan, "Linear systems with state and control constraints: the theory and application of maximal output admissible sets," IEEE Trans. Automat. Contr., vol. 36, no. 9, pp. 1008-1020, Sep. 1991.